

Chapter 26

Simulation of High-Temperature Solid Particle Erosion of HVOF-Sprayed NiCrBSiFe and WC-Co/NiCrBSiFe-Coated Wall Using CFD



K. Raghavendra Naik, R. K. Kumar, V. Saravanan, S. Seetharamu and P. Sampathkumar

Abstract The erosion characteristics of HVOF-sprayed NiCrBSiFe and WC-Co/NiCrBSiFe coatings made on SS347 grade steel have been investigated for high-temperature behaviour, especially in the boiler tubes used in thermal power generation. The computational fluid dynamic model has been adopted to study the influence of the impingement angle on the erosion properties of the coatings. The self-fluxing NiCrBSiFe alloys have shown the best erosion resistance of about two times at room temperature and about four times at 700 °C when compared with a composite powdered coating of WC-Co/NiCrBSiFe. At 700 °C, The WC-Co/NiCrBSiFe undergoes thermal cracking between nickel rich and WC metallic phases due to low oxidation and thermal expansion mismatch between them leading to degradation of the coating; however, at this temperature, the self-fluxing alloy of NiCrBSiFe performed better when compared to WC-Co/NiCrBSiFe coating. The simulation is done with turbulence model, namely shear stress transport (SST) model with a base on user-defined function predicted from the experimental results. The computational fluid dynamic simulated data obtained from SST model and the experimental results were compared, and they are in good agreement with each other.

Keywords Erosion rate · Solid particle impact · Coatings · Computational fluid dynamics (CFD) · SST turbulence model

K. Raghavendra Naik (✉) · R. K. Kumar · V. Saravanan
Material Technology Division, Central Power Research Institute, Bengaluru 560080, India
e-mail: raghavendranaik454@gmail.com

S. Seetharamu
Department of Mechanical Engineering, Nitte Meenakshi Institute of Technology,
Bengaluru 560064, India

P. Sampathkumar
Department of Mechanical Engineering, Sambhram Institute of Technology,
Bengaluru 560097, India

© Springer Nature Singapore Pte Ltd. 2020
M. Vinyas et al. (eds.), *Advances in Structures, Systems and Materials*,
Lecture Notes on Multidisciplinary Industrial Engineering,
https://doi.org/10.1007/978-981-15-3254-2_26

26.1 Introduction

Solid particle erosion is a serious problem in power plants, which reduces the service life of the mechanical components operating at high temperature due to impingement of coal and ash particles [1–3]. For instance, boiler tubes undergo severe degradation due to impaction of ash particles, containing quartz leading to the forced shutdown of the plant [4, 5]. The coating has been proven to be one of the advanced methods employed to set the best erosion resistance due to solid particle impact. There are several methods of deposition process known, and it is dependent on the type of application. For example, the coating processes such as weld overlay, thermal spray, diffusion, laser cladding, etc., adopted in thermal power plants face certain drawbacks such as very thin coatings are possible in the diffusion process, embrittlement taking place at the interface due to repeated welding and leading to crack formation in weld overlay and very difficult to repair or refurbish at site. In view of the problem faced in this process, thermal spray coating gains momentum [6, 7] as they overcome them.

The factors like hardness, velocity, impingement angle, size and shape of the erodent need to be considered to study the erosion behaviour in detail both at room and elevated temperature among them; velocity and impact angle play a major role in selecting the coatings [8]. As per the theoretical predictions, ductile materials erode more rapidly at shallow impact angle (10° – 30°); however, brittle material erodes more at normal impact angle (70° – 90°) [9, 10]. The erosion rate at elevated temperatures is much higher at shallow as well as at normal impact angles compared to the room temperature erosion [11].

The high-velocity oxy-fuel (HVOF) process comes under the thermal spray, and it is being deployed in industries effectively from the point of erosion protection. The advantages of this spraying process are that it yields lower porosity levels, higher density, lower oxide content and superior bond strength compared to the conventional coatings [12].

Self-fluxing thermal spray coating like Ni-base will provide high erosive wear resistance at low and moderate temperature, and hence, it has received widespread applications [13]. The distributed hard WC particles in the Ni matrix will increase the hardness of the coating, thereby improving the erosion resistance at a higher temperature. The published information on 35% WC with NiCrBSiFe has shown superior wear resistance up to 500 °C in view of higher hardness and minimal porosity level achieved [14–16]. In the present study, an attempt has been made on the wear characteristics evaluation beyond 500 °C.

In recent trends, computational fluid dynamic (CFD) approach has become a useful tool to assess the erosion rate both at room and high temperature, and many works have been reported on this to account for the elevated temperature erosion behaviour of bulk material and coatings. The experimental data, therefore, serves as a validation tool to predict erosion behavior computationally. Thus, CFD is one of the advanced methods employed to predict the erosion phenomena for different flow conditions both at room temperature and high-temperature regimes. The CFD approach in conjunction with experimental data has been effectively used [17–21]

to study the wall thinning of pipes in the pulverised fuel system, slurry and silt erosion, ash erosion in pressure parts, etc., evolving amicable solutions to the critical problems faced in thermal power plants.

The published information on the topic (up to 800 °C) for plasma-sprayed coating with lower velocity of about 4 m/s indicates lower erosion of NiCrBSi and highest erosion of WC-CO/NiCrBSi. However, in the present work, the attempt has been made with HVOF self-fluxing alloy of NiCrBSiFe and the distributed hard 35% WC particles in the nickel matrix with high velocity up to 36 m/s, which simulating boiler environment and compared the erosion rate intensity through CFD modelling.

26.2 Experimentation

26.2.1 Materials and Methods

The SS-347 steel is the substrate material used as this finds extensive applications in a pulverised coal-fired thermal power plant. The coatings were made with a velocity of 680 m/s on the SS-347 base material of size $150 \times 150 \times 7 \text{ mm}^3$. The test samples of size $15 \times 15 \times 7 \text{ mm}^3$ were prepared using electro-discharge machining cutting process for testing and microstructural examination. The regular metallurgical procedure has been adopted for polishing and etching. The input conditions employed in the coating process and powder coating details are shown in Tables 26.1 and 26.2.

26.2.2 Erosion Test at Elevated Temperature

An erosion test set-up was designed and built to achieve the real service condition experienced in boiler involving high temperature as shown in Fig. 26.1. The morphology of erodent, namely silica sand, is shown in Fig. 26.2. The erosion test was

Table 26.1 HVOF spray parameter

Powder: Praxair 1350 VM size: -45 to $+15 \mu\text{m}$, JP5000HVOF		
1	Type of fuel: kerosene @ 170 PSIG, SCFH	5.8
2	The flow rate of oxygen @ 210 PSIG, SCFH	1850
3	Distance between nozzle to target, metre	0.381
4	Nitrogen as carrier gas @ 50 PSIG, SCFH	23
5	The velocity of particle pertaining to spray, m/s	680 ^a
6	Per pass thickness of deposit formed	15
7	The feed rate of powder, kg/min	0.09

^aProvided by the supplier of the coating

Table 26.2 Powder coating details

Code of sample	Chemical composition (weight percentage) of coating	Range of powder size (μm)
D1	NiCrBSiFe (14.7 Cr-3.21 B-4.35 Si-3.75 Fe-Bal-Ni)	-45 to +15
N1	35 WC-Co/65 NiCrBSiFe (30.6 W-4.2 Co-10.4 Cr-47.6 Ni-1.8 B-2.6 Si-2.8 Fe)	-45 to +15

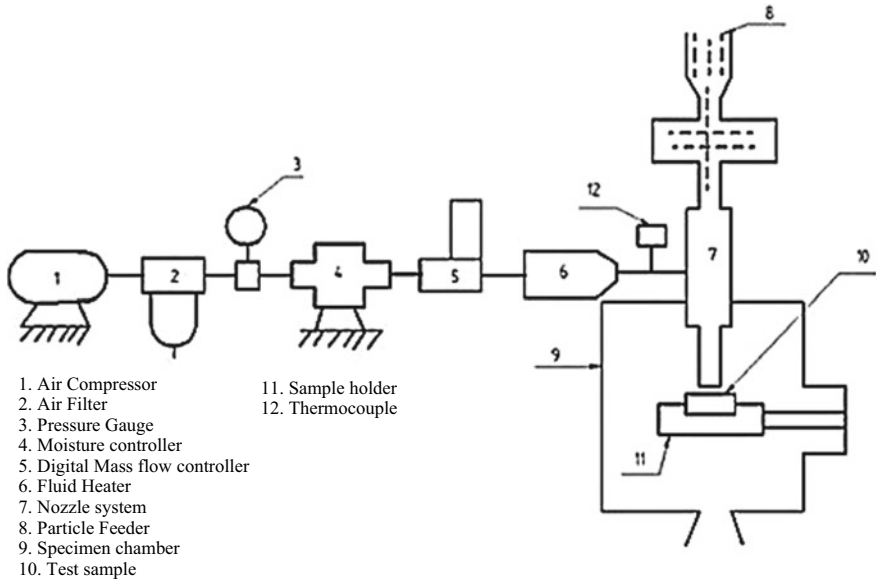


Fig. 26.1 High-temperature erosion test rig diagram

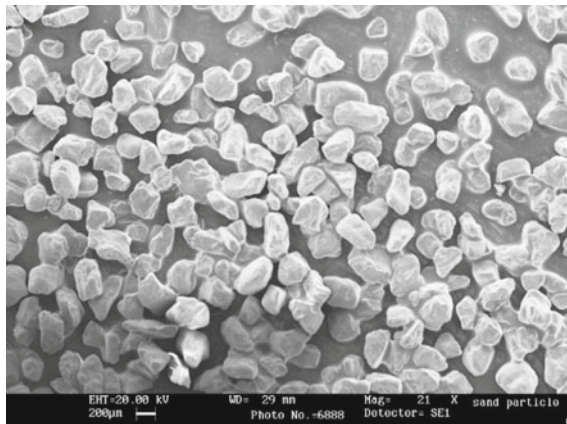


Fig. 26.2 Structure of erodent (silica sand)

conducted with the target sample fixed in a holder, which can be moved to set the desired impact angle of 15°, 30°, 45°, 75° and 90° which has been on the varying intensity levels of damage from the leading edge to the trailing edge. This is an accelerated test with the oil- and moisture-free dry air obtained from a compressor. Dry air is mixed with silica sand and then made to impinge on the sample to study the erosion behaviour both at room temperature and high temperature (700 °C). The particle velocity has been measured using double-disc device [22]. Table 26.3 gives the input parameters employed in this work.

26.2.3 Microstructure Observations

Figures 26.3 and 26.4 show the microstructure of the typical cross section of the

Table 26.3 Erosion test conditions

1	Abrasive type	Silica sand
2	Particle size	70 AFS
3	Particle velocity	36 m/s
4	Feed rate	142 g/min
5	Impingement angle	90° and 30°
6	Test temperature	Ambient temperature and high temperature (700 °C)
7	Test duration	7 min
8	Test specimen size	25 × 25 × 7 mm
9	Diameter of nozzle	5 mm

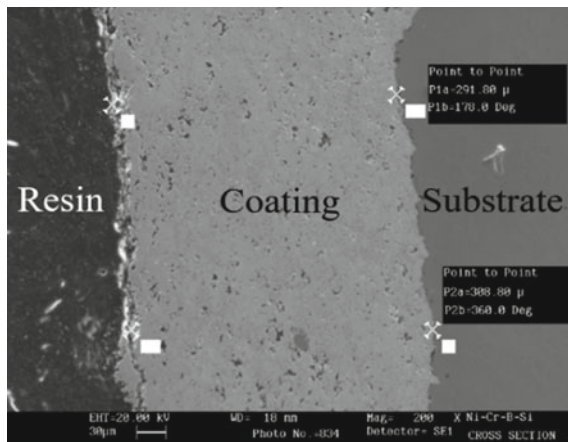
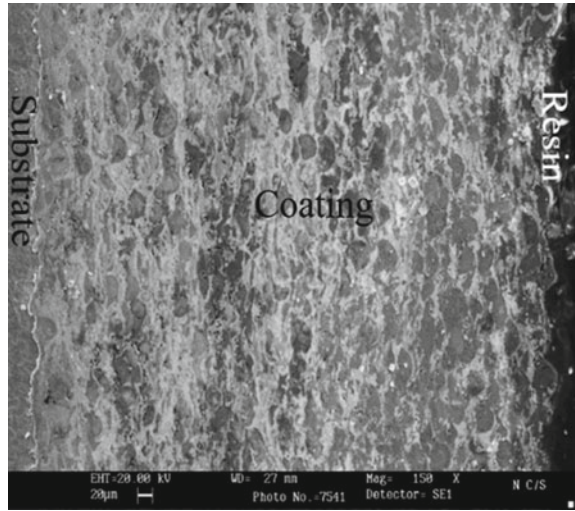


Fig. 26.3 Cross section of as-sprayed NiCrBSiFe

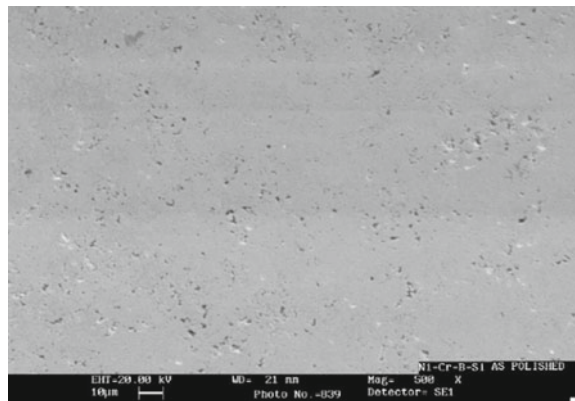
Fig. 26.4 Cross section of as-sprayed 35 WC-Co/NiCrBSiFe



D1- and N1-sprayed HVOF sample. The purpose of adding WC to the matrix is to enhance the hardness level. The microhardness and the porosity were measured for both coatings. D1 coating shows the hardness and porosity level of about 750 HV_{0.3} and 2.1%, for N1 coating, hardness of about 1050 HV_{0.3} and 3.0% porosity, respectively.

The surface morphology of the D1 and N1 coatings is as shown in Figs. 26.5 and 26.6. From the surface morphology of the coating, it is observed that there is a higher porosity level in N1 coating. The dispersion of WC in the nickel-rich matrix in N1 coating increases the porosity level when compared to D1 coating, which may result in an increase in stress level around the pores. As the particle interact the surface, the cracks nucleate and propagate easily and cause the material to come off easily, thus resulting in higher erosion loss of the coating and also at 700 °C; the hardness

Fig. 26.5 SEM morphology of surface as-sprayed NiCrBSiFe



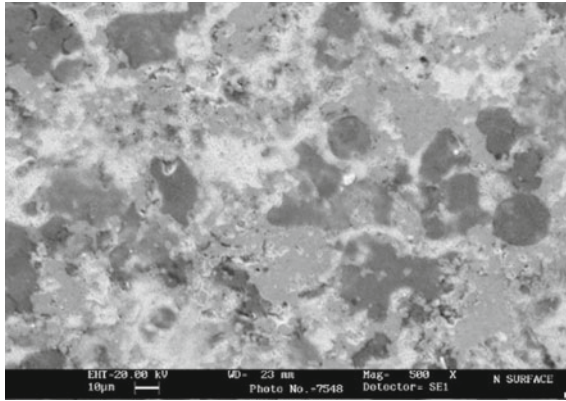


Fig. 26.6 SEM morphology of surface as-sprayed 35 WC-Co/NiCrBSiFe

decreases and hence results in higher erosion loss; similar observations have been made by other researchers reported [23, 24].

26.3 CFD Erosion Simulation

The CFD approach has been adopted to identify the critical erosion-prone regions obtaining low, mild and high erosion regions based on the varied flow conditions, flow trajectories, varied impact angles keeping the solid burden constant (gram loss per kg of abrasive used).

The individual model has been developed for five different impact angles of 15°, 30°, 45°, 75° and 90° to get particle trajectories and averaged particle impact velocity, but in this work, only the impact angles of 30° and 90° are considered for this study; following this, the simulation work has been done, and the data have been generated.

26.3.1 Development of Erosion Model for Prediction of Erosion Rate

In the erosion model, material removal takes place mainly by the impact of erodent particles on the target material due to the high kinetic energy possessed by the particle transforming it to potential energy. The erosion phenomena being complex in nature follow a particular sequence; the erosion loss governs the following equation.

$$E = K \cdot V_p^n \cdot (\alpha)^M \cdot \dot{m} \quad (26.1)$$

Table 26.4 Multiple nonlinear regression analysis data

Temperature (°C)	Materials	K	n	M
RT/Ambient	D1	3.01e-11	1.69	0.334
RT/Ambient	N1	8.76e-12	2.52	0.647
700	D1	1.911e-9	0.928	0.283
700	N1	2.586e-9	0.987	0.5547

where

V_p	particle impact velocity
K	constant reference velocity factor
α	impact angle in radian
n, M	velocity and angle exponent
\dot{m}	mass flow rate of erodent impacting
V_o	reference velocity
V_o	$(1/k^{1/n})$
Erosion rate/ \dot{m}	$(V_p/V_o)^n (\alpha)^M$

The impact angle is expressed in radians, and it is the angle between the approaching particle track and the wall. The experimental values with velocity, impact angle and temperature ranges are taken to MATLAB to solve multiple nonlinear regression analysis and the values of K , n and M are obtained by curve fit as shown in Table 26.4.

The above erosion Eq. (26.1) is implemented in Fortran code, with the help of Ansys CFX. Fortran subroutine is created in the form of user routine and finally source code Pt_erosion. F is called for solutions to the erosion equation for each of the material D1 and N1. A user-defined function is derived to solve the erosion equation which consists of velocity, impact angle, impact location and temperature of the target surface.

The sieve analysis is carried out to determine the particle size and its distribution, and for CFD analysis, the following assumptions have been made

1. The shape factor assumed to be 0.75
2. Particle impact is inelastic in nature
3. Perpendicular and parallel coefficient is considered as one

Also, three different velocities (20, 26 and 36 m/s) are considered in this, and the gap maintained between the jet and the test sample is 10 mm.

26.3.2 CFD Turbulence Model

Turbulence models are generally considered to predict the flow patterns. The shear stress transport model (SST) is nothing but two equations model which is more advanced than zero equation model [25]. The SST model is robust, and accuracy is

good when compared with the other models like $k\text{-}\epsilon$, $k\text{-}\omega$ and SSG Reynolds stress model. In the present CFD work, SST model has been used in view of possessing a higher accuracy level.

26.3.2.1 SST (Shear Stress Transport) Model

The SST model is developed by Menter [26] and designed by Wilcox [27]. This model is a combination of the conventional k-epsilon and k-omega model.

$$\omega = \frac{k}{V_t}$$

In the SST model, turbulence viscosity V_t is defined as

$$V_t = \frac{a_1 k}{\max(a_1 \omega, \Omega F_2)}$$

where a_1 is the 0.30 coefficient; the absolute value of the vorticity Ω is

$$F_2 = \tan h \left[\left[\max \left(2\sqrt{k}/0.09 \omega y, 500 \nu/\omega y^2 \right) \right]^2 \right]$$

where y is the distance from the nearest wall, and ν is the kinematic viscosity.

26.3.3 Model Description

There is a total mesh of 2,62,317 nodes and 2,80,666 elements. Ansys CFX15 is used to perform CFD analysis. Ansys-Pre was used to mesh 3D structures, as shown in Fig. 26.7a. The target surface and near-wall are used to have finer meshes with the dominant mesh of hexahedron. The hexahedron-based fluid mesh gives good results

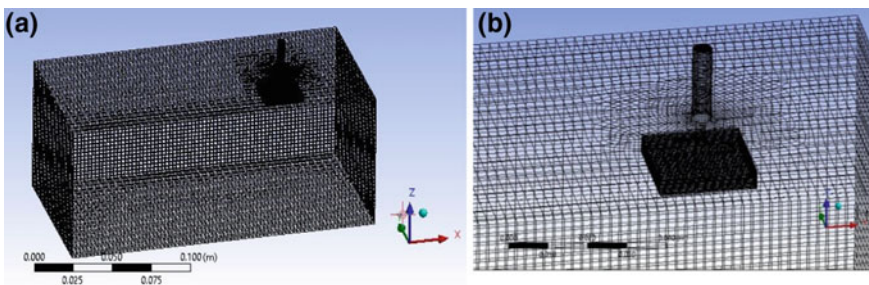


Fig. 26.7 Generation of mesh **a** domain of control volume **b** specimen to target surface

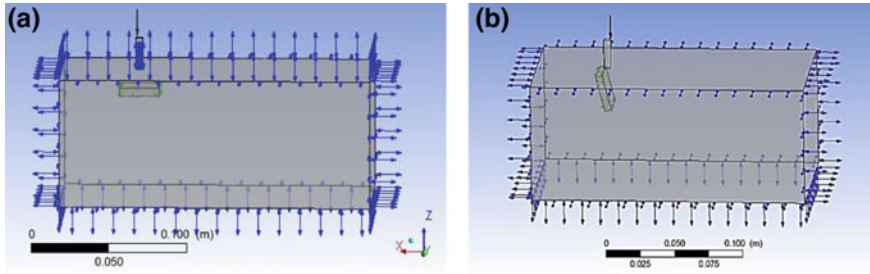


Fig. 26.8 Geometrical model set-up used for CFD study

Table 26.5 Boundary conditions adopted for CFD simulation study

Inflow condition	The mass flow rate of erodent and air velocity
Target surface	No-slip conditions
Roughness of wall	As-polished condition
Turbulence model	SST model standard
Outlet condition	Atmospheric pressure conditions with opening boundary

in analysing fluid flow near the target wall, as shown in Fig. 26.7b. The SST model involving steady state is used to simulate the flow conditions and codes developed using subroutine in the calculation part of erosion rate where the particle flow is in the opposite of the Z direction.

Figure 26.8 a and b shows the model with an impact angle of 90° and 30°. The boundary conditions adopted during CFD simulation are shown in Table 26.5.

26.4 Results and Discussion

26.4.1 CFD Simulation Results

The velocity of the particle to predict the erosion behaviour is 36 m/s and it is arrived at based on the experiments. The solid particle vectors contours is shown in Fig 26.9.

Figure 26.10 shows the distribution of erosion rate density of the sample of both D1 and N1 coatings at 30° and 90° impact angle using the SST turbulence model. The erosion scars from the CFD prediction replicate similar to the experimental test scar as shown in Fig. 26.11.

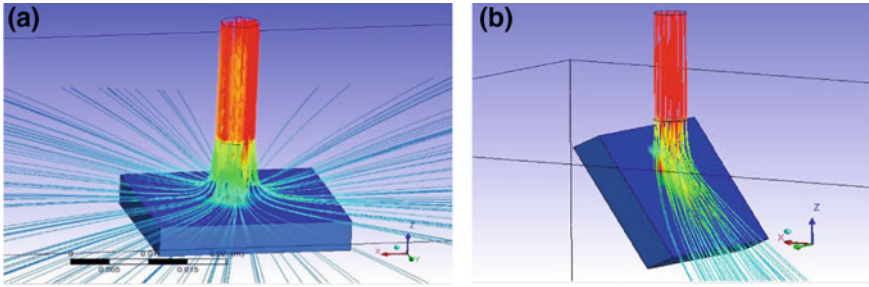


Fig. 26.9 Erosion rate density of contour **a** 90° **b** 30° impact angle

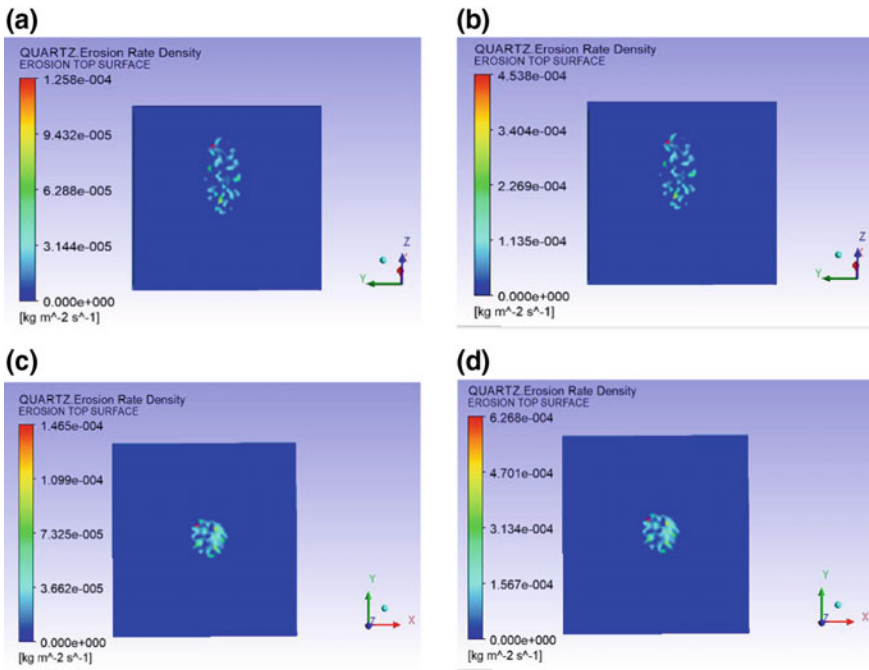


Fig. 26.10 Erosion rate density distribution on the target surface of the specimen **a** D1 **b** N1 at 30° impact angle and **c** D1 **d** N1 at 90° impact angle at a temperature of 700 °C

26.4.2 Discussion

Erosion Mechanism: The erosion rate of the self-fluxing alloy (single metallic coating) of D1 and N1 (two-phase materials) coatings with the impact angle of 30° and 90° for room and elevated temperature (700 °C) is shown in Fig. 26.12.

Figure 26.12 gives the erosion rate versus the impact angle. At room temperature, both coatings D1 and N1 show superior erosion resistance; however, at 90° impact,

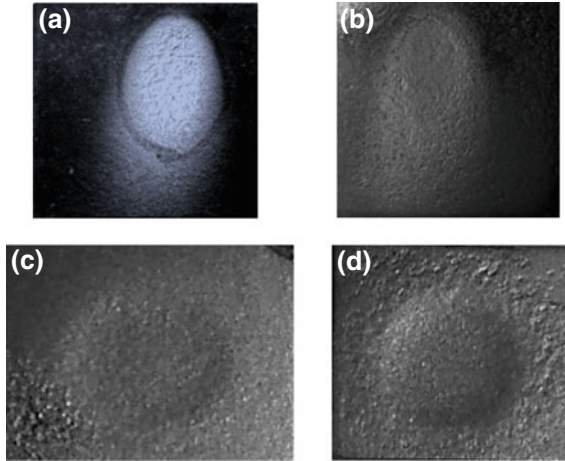


Fig. 26.11 Erosion rates on the target surface of specimen **a** D1 **b** N1 at 30° impact angle and **c** D1 **d** N1 at 90° impact angle at a temperature of 700 °C

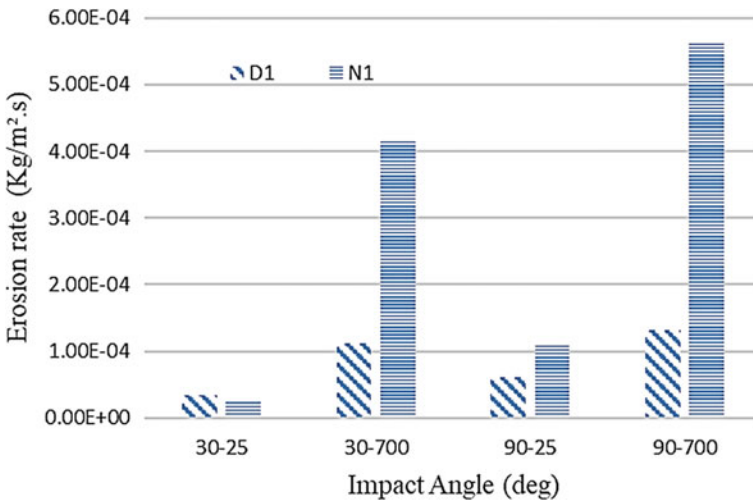


Fig. 26.12 Histogram illustrating the room and high-temperature erosion rate of D1 and N1 coatings at two different impact angles of 30° and 90°

the erosion is higher for both coatings; this may be due to brittle erosion nature at normal impact angle.

In the case of D1 coating at a higher temperature of 700 °C, the erosion rate is decreased at both the shallow and normal impact angle. At shallow impact angle coating will undergo plastic deformation as the material removal is by cutting and ploughing mechanisms, whereas at a higher angle of 90°, the erosion damage takes

place due to the repeated impact of the erodent. In this case, the erosion mechanism may be a combination of grooving, cratering and microcracking. The microstructure of the D1 coating has dense and layered structure and the microhardness of the coating measured is 780 HV. When the coating is exposed to higher temperatures, the hardness of the coating is reduced to half (430 HV) the value measured at room temperature. Even though the coating can withstand erosion at high temperatures, it is likely that there is an improvement in toughness due to the drop in hardness. It is well known that when the hardness decreases, the toughness increases [24].

In the case of N1 coating at a higher temperature of 700 °C, the rate of erosion is less at 30° impact and more at normal impact angle which is a characteristic behaviour of brittle materials. When the WC content in the coatings varies from 0 to 18%, the coating hardness increases gradually; however, with the increase of WC content, the porosity level also increases which leads to larger pores. When the WC content is more (35%), the brittleness as well as the pore size increases predominantly. These bigger sized pores may provide a path for the fracture and lead to the propagation of the crack. If the WC content is less than 25%, the pore sizes are smaller resulting in crack not getting formed as it absorbs a larger amount of impact energy. Further, a higher amount of WC (35%) with large pores undergoes the higher amount of plastic deformation with the formation of network cracks and gives rise to ease pathway by the crack propagation to occur. In the process, surface layer comes off following the delamination theory. The hardness of the coating by the addition of 35% WC was 1056 HV by exposing to a higher temperature of 700 °C; the hardness of the coating was reduced to 520 HV (almost half) which causes the highest erosion rate; lower hardness results in poor erosion resistance.

The erosion rate at an elevated temperature at normal impact angle was nearly 5–6 times higher for both the coating tested. Compared to stainless steel and other NiCr alloys, NiCrBSiFe coating has been proven to be very promising. WC agreements the greater wear resistance at room temperature; however, its poor resistance to oxidation and thermal expansion mismatch restricts its application to a temperature above 450–550 °C; similar kind of observation has been reported elsewhere [28–30], and the erosion loss governs Eq. (26.1) which is as per the literature [31].

26.4.3 Assessment of Simulation and Experimental Results

The erosion rate of D1 and N1 coatings for room and high temperature is shown in Table 26.6. The average erosion rate on the target surfaces of the specimen through experiments and computer simulation using the SST model is also shown. The SST model belongs to the family of eddy dissipation model and has been chosen because of its high accuracy and accurate prediction of flow separation from a smooth surface at the time of particle impact; similar kind of prediction is reported [25].

In this context, it is worth mentioning here that the work carried out by Kim et al. [21] has adopted the SST model for solid particle erosion prediction and compared it with the *k*-epsilon model and reported that the SST model is much better compared

Table 26.6 Comparison of experimental and simulation results on erosion

Sample	Impact angle (°)	Experimental data (kg/m ² s)	Numerical data (kg/m ² s)	% error
D1-25	30	3.50e-5	3.89e-5	11.13
N1-25	30	2.78e-5	3.16e-5	13.67
D1-700	30	1.12e-4	1.25e-4	11.60
N1-700	30	4.15e-4	4.54e-4	9.56
D1-25	90	6.09e-5	6.83e-5	12.11
N1-25	90	1.11e-4	1.21e-4	9.00
D1-700	90	1.32e-4	1.46e-4	10.98
N1-700	90	5.65e-4	6.28e-4	11.23

to the other models. Hence, in the present investigation, also SST model is used to the advantage of predicting the erosion rate in WC-nickel target material with minimum acceptable error. Further, it is seen that the % error (Table 26.6) obtained between the experiments and SST simulation lies in the range 9–14% which seems to be in the acceptable range. Thus, it is summarized both the experimental and simulated results are in close agreement with each other.

26.5 Conclusions

The experimental results pertaining to erosion characteristics at elevated temperature of self-fluxing NiCrBSiFe alloy and 35% WC-Co/NiCrBSiFe coatings made by HVOF technique have been investigated and compared with the CFD numerical simulation model. The CFD data closely match the experimental values obtained. The following are the important conclusions drawn.

- The HVOF-sprayed NiCrBSiFe-coated samples have shown higher erosion resistance both at room temperature and elevated temperature (700 °C) compared to 35% WC-Co/NiCrBSiFe HVOF-coated sample irrespective of the impact angle.
- It is desirable to adopt NiCrBSiFe coating for high-temperature erosion application as it does not seem to undergo oxidation.
- It is preferable to use WC-Co/NiCrBSiFe coating at a shallow angle (20°–30°) for erosion resistance application at room temperature, but at 90° impact angle, NiCrBSiFe is preferable.
- The percentage error obtained between the experimental results and CFD simulated data lies in the range 9% to 14%, which seems to be in the acceptable limits.
- The CFD application with the SST model seems to predict the erosion behaviour better using Ansys CFX module and the same study may be extended to higher temperature (greater than 700 °C) regimes.

Acknowledgements The authors wish to thank profoundly the management of CPRI for according permission to publish this paper. This paper is a part of a bigger project which was under the research contingency (RC) funding.

References

1. Ramesh, C.S., Seshadri, S.K., Iyer, K.J.: A survey of aspects of wear of metals. *Indian J. Technol.* **29**(4), 179–185 (1991)
2. Archer, N.J., Yee, K.K.: Chemical vapour deposited tungsten carbide wear-resistant coatings formed at low temperatures. *Wear* **48**(2), 237–250 (1978)
3. Pawlowski, L.: *The Science and Engineering of Thermal Spray Coatings*. Wiley & Sons, 30 Apr 2008
4. Uusitalo, M.A., Vuoristo, P.M., Mäntylä, T.A.: High-temperature corrosion of coatings and boiler steels in the oxidizing chlorine-containing atmosphere. *Mater. Sci. Eng.* **346**(1–2), 168–177 (2003)
5. Stultz, S.C., Kitto, J.B. (eds.): *Steam: Its Generation and Use*. Babcock and Wilcox, Barberton, OH (1992)
6. Uusitalo, M.A., Vuoristo, P.M., Mäntylä, T.A.: High-temperature corrosion of coatings and boiler steels below chlorine-containing salt deposits. *Corrosion Sci.* **46**(6), 1311–1331 (2004)
7. Miguel, J.M., Guilemany, J.M., Vizcaino, S.: Tribological study of NiCrBSi coating obtained by different processes. *Tribol. Int.* **36**(3), 181–187 (2003)
8. Hutchings, I.M.: Wear by particulates. *Chem. Eng. Sci.* **42**(4), 869–878 (1987)
9. Sundararajan, G.: A comprehensive model for the solid particle erosion of ductile materials. *Wear* **149**(1–2), 111–127 (1991)
10. Finnie, I.: In: Nateson, K. (ed.) *Corrosion-Erosion Behavior of Materials*, p. 437. AIME, New York (1980)
11. Kulu, P., Hussainova, I., Veinthal, R.: Solid particle erosion of thermal sprayed coatings. *Wear* **258**(1–4), 488–496 (2005)
12. Mohanty, M., Smith, R.W., De Bonte, M., Celis, J.P., Lugscheider, E.: Sliding wear behaviour of thermally sprayed 75/25 Cr₃C₂/NiCr wear resistant coatings. *Wear* **198**(1–2), 251–266 (1996)
13. Kim, H.J., Hwang, S.Y., Lee, C.H., Juvanon, P.: Assessment of wear performance of flame sprayed and fused Ni-based coatings. *Surf. Coat. Technol.* **172**(2–3), 262–269 (2003)
14. Bell, G.R.: Eighth International Thermal Spraying Conference, Mimi, Florida, USA, pp. 396–406 (1976)
15. Ding, Z., Knight, R., Smith, R.W.: *Thermal Spray: A United Forum for Scientific and Technological Advances*, Materials Park, Ohio, USA, pp. 91–95 (1997)
16. Heath, G.R., Kamer, P.A.: *Surface Modification Technology IX*, Cleveland, Ohio, USA, pp. 109–113 (1995)
17. Parsi, M., Agrawal, M., Srinivasan, V., Vieira, R.E., Torres, C.F., McLaury, B.S., Shirazi, S.A.: CFD simulation of sand particle erosion in gas-dominant multiphase flow. *J. Nat. Gas Sci. Eng.* **27**, 706–718 (2015)
18. Duarte, C.A., de Souza, F.J., de Vasconcelos Salvo, R., dos Santos, V.F.: The role of inter-particle collisions on elbow erosion. *Int. J. Multiph. Flow* **89**, 1–22 (2017)
19. Zahedi, P., Zhang, J., Arabnejad, H., McLaury, B.S., Shirazi, S.A.: CFD simulation of multiphase flows and erosion predictions under annular flow and low liquid loading conditions. *Wear* **376**, 1260–1270 (2017)
20. Gandhi, M.B., Vuthaluru, R., Vuthaluru, H., French, D., Shah, K.: CFD based prediction of erosion rate in large scale wall-fired boiler. *Appl. Therm. Eng.* **42**, 90–100 (2012)
21. Kim, J.H., Joo, H.G., Lee, K.Y.: Simulation of solid particle erosion in WC-Ni coated wall using CFD. *J. Mater. Process. Technol.* **224**, 240–245 (2015)

22. Ruff, A.W., Ives, L.K.: Measurement of solid particle velocity in erosive wear. *Wear* **35**, 195–199 (1975)
23. Hidalgo, V.H., Varela, F.B., Menéndez, A.C., Martínez, S.P.: A comparative study of high-temperature erosion wear of plasma-sprayed NiCrBSiFe and WC–NiCrBSiFe coatings under simulated coal-fired boiler conditions. *Tribol. Int.* **34**(3), 161–169 (2001)
24. Tu, J.P., Liu, M.S., Mao, Z.Y.: Erosion resistance of Ni–WC self-fluxing alloy coating at high temperature. *Wear* **209**(1–2), 43–48 (1997)
25. Sklavounos, S., Rigas, F.: Validation of turbulence models in heavy gas dispersion over obstacles. *J. Hazard. Mater.* **108**(1–2), 9–20 (2004)
26. Menter, F.R.: Two-equation eddy-viscosity turbulence models for engineering applications. *AIAA J.* **40**(2), 254–266 (2002)
27. Wilcox, D.C.: Reassessment of the scale-determining equation for advanced turbulence models. *AIAA J.* **26**(11), 1299–1310 (1988)
28. Russo, L., Dorfman, M.: A structural evaluation of HVOF sprayed NiCr–Cr sub 3 C sub 2 coatings. *Therm. Spray. Curr. Status Futur. Trends* **2**, 681–686 (1995)
29. Berger, L.M., Hermel, W., Vuoristo, P., Mantyla, T., Lengauer, W., Etmayer, P.: Structure, properties and potentials of WC–Co, Cr₃C₂–NiCr and TiC–Ni-based hard metal like coatings. In: Berndt, C.C. (ed.) *Thermal Spray: Practical Solutions for Engineering Problems*, pp. 89–98 (1996)
30. Berger, Z., Livshitz, M.: The structure and properties of hypervelocity oxy-fuel (HVOF) sprayed coatings. *High-Temp. Mater. Process.* **15**, 179–186 (1996)
31. Raask, E.: *Mineral Impurities in Coal Combustion: Behaviour, Problems, and Remedial Measures*. Taylor & Francis (1985)